

Genome-wide identification and analysis of cystatin family genes in Sorghum (*Sorghum bicolor* L.)

Jie Li¹, Xinhao Liu², Jingmei Wang², Junyan Sun¹, Dexian He^{Corresp. 3}

¹ College of Agronomy, Xinyang Agriculture and Forestry University, Xinyang, Henan Province, China

² Central Laboratory, Xinyang Agriculture and Forestry University, Xinyang, Henan Province, China

³ Collaborative Innovation Center of Henan Grain Crops/National Key Laboratory of Wheat and Maize Crop Science, College of Agronomy, Henan Agricultural University, Zhengzhou, China

Corresponding Author: Dexian He
Email address: hedexian@126.com

To set a systematic study of the Sorghum *cystatins* (*SbCys*) gene family, a comprehensive genome-wide analysis of the *SbCys* family genes was performed by bioinformatics-based methods. In total, 18 *SbCys* genes were identified in Sorghum, which were distributed unevenly on chromosomes, and two genes were involved in a tandem duplication event. All *SbCys* genes had similar exon/intron structure and motifs, indicating their high evolutionary conservation. Transcriptome analysis showed that 16 *SbCys* genes were expressed in different tissues, and most genes displayed higher expression levels in reproductive tissues than in vegetative tissues, indicating that the *SbCys* genes participated in the regulation of seed formation. Furthermore, the expression profiles of the *SbCys* genes revealed that 7 cystatin family genes were induced during *Bipolaris sorghicola* infection and only 2 genes were responsive to aphid infestation. In addition, quantitative real-time polymerase chain reaction (qRT-PCR) confirmed that 17 *SbCys* genes were induced by one or two abiotic stresses (dehydration, salt, and ABA stresses). The interaction network indicated that *SbCys* proteins were associated with several biological processes, including seed development and stress responses. Notably, the expression of *SbCys4* was up-regulated under biotic and abiotic stresses, suggesting its potential roles in mediating the responses of Sorghum to adverse environmental impact. Our results provide new insights into the structural and functional characteristics of the *SbCys* gene family, which lay the foundation for better understanding the roles and regulatory mechanism of Sorghum cystatins in seed development and responses to different stress conditions.

1 Genome-wide identification and analysis of cystatin family genes
2 in Sorghum (*Sorghum bicolor* L. Moench)

3 Jie Li¹, Xinhao Liu², Jingmei Wang², Junyan Sun¹, Dexian He^{3*}

4

5 **Author affiliation:**

6 1 College of Agronomy, Xinyang Agriculture and Forestry University, Xinyang, Henan 464001,
7 China

8 2 Central Laboratory, Xinyang Agriculture and Forestry University, Xinyang, Henan 464001,
9 China

10 3 Collaborative Innovation Center of Henan Grain Crops/National Key Laboratory of Wheat and
11 Maize Crop Science, College of Agronomy, Henan Agricultural University, Zhengzhou, Henan,
12 450002, China

13

14 *Corresponding author: Dexian He

15 College of Agronomy, Henan Agricultural University, Zhengzhou, Henan, 450002, China

16 E-mail: hedexian@126.com

17

18

19

20

21

22

23

24 **ABSTRACT**

25 To set a systematic study of the Sorghum *cystatins* (*SbCys*) gene family, a comprehensive
26 genome-wide analysis of the *SbCys* family genes was performed by bioinformatics-based
27 methods. In total, 18 *SbCys* genes were identified in Sorghum, which were distributed unevenly
28 on chromosomes, and two genes were involved in a tandem duplication event. All *SbCys* genes
29 had similar exon/intron structure and motifs, indicating their high evolutionary conservation.
30 Transcriptome analysis showed that 16 *SbCys* genes were expressed in different tissues, and most
31 genes displayed higher expression levels in reproductive tissues than in vegetative tissues,
32 indicating that the *SbCys* genes participated in the regulation of seed formation. Furthermore, the
33 expression profiles of the *SbCys* genes revealed that 7 cystatin family genes were induced during
34 *Bipolaris sorghicola* infection and only 2 genes were responsive to aphid infestation. In addition,
35 quantitative real-time polymerase chain reaction (qRT-PCR) confirmed that 17 *SbCys* genes
36 were induced by one or two abiotic stresses (dehydration, salt, and ABA stresses). The
37 interaction network indicated that *SbCys* proteins were associated with several biological
38 processes, including seed development and stress responses. Notably, the expression of *SbCys4*
39 was up-regulated under biotic and abiotic stresses, suggesting its potential roles in mediating the
40 responses of Sorghum to adverse environmental impact. Our results provide new insights into the
41 structural and functional characteristics of the *SbCys* gene family, which lay the foundation for
42 better understanding the roles and regulatory mechanism of Sorghum cystatins in seed
43 development and responses to different stress conditions.

44 **INTRODUCTION**

45 Cystatins are competitive and reversible inhibitors of cysteine proteases from families C1A and

46 C13, which have been identified in many plant species (Martinez and Diaz, 2008; Zhao et al.
47 2014). Cystatins are categorized into three groups, including stefins without disulfide bonds
48 (Group I), cystatins with four conserved Cys residues forming two disulfide bonds (Group II),
49 and kininogens with repeated, stefin-like domains (Group III) (Meriem et al. 2010). Cystatins are
50 widely distributed in animal and plant systems (Tremblay et al. 2019). Based on their primary
51 sequence homology, cystatins contain three signature motifs including a QxVxG reactive site, a
52 tryptophan residue (W) located downstream of the reactive site, and one or two glycine (G)
53 residues in the flexible N terminus of the protein. These three motifs are important for the
54 cystatin inhibitory mechanism (Martinez et al. 2009). In addition, a consensus sequence ([LVI]-
55 [AGT]-[RKE]-[FY]-[AS]-[VI]-x-[EDQV]-[HYFQ]-N) in cystatins is conformed to a predicted
56 secondary α -helix structure (Meriem et al. 2010). Most plant cystatins are small proteins with a
57 molecular mass in the 12- to 16-kD range (Meriem et al. 2010). Some plant cystatins contain a
58 C-terminal extension that raises their molecular weights up to 23 kDa. The longer C-terminal
59 extensions are thought to be involved in the inhibition of cysteine protease activities in the
60 peptidase C13 family (Martinez et al. 2007; Martinez and Diaz, 2008).

61 The principal functions of plant cystatins are related to the regulation of endogenous cystein
62 proteases during plant growth and development, senescence, and programmed cell death
63 (Belenghi et al. 2010; Díazmendoza et al. 2014; Zhao et al. 2014). Additionally, plant cystatins
64 have been used as effective molecules against different pests and pathogens (Martinez et al.
65 2016). For example, several publications reported the inhibition of recombinant cystatins on the
66 growth of some pests and fungi (Lima et al. 2015; Tremblay et al. 2019). Tomato plants over-
67 expressing the wheat cystatin *TaMDC1* displayed a broad stress resistance to bacterial pathogen,
68 and the defense responses were mediated by methyl jasmonate and salicylic acid (Christova et al.

69 2018). The inhibition of amaranth cystatin on the digestive insect cysteine endopeptidases was
70 observed by Valdés-Rodríguez et al. (2015). Plant cystatins are also involved in the responses to
71 abiotic stresses, such as over-expression of *MpCYS4* in apple delayed natural and stress-induced
72 leaf senescence (Tan et al. 2017). Song et al. (2017) found that the expression of *AtCYS5* was
73 induced by heat stress (HS) and exogenous ABA treatment in germinating seed, furthermore,
74 over expression of *AtCYS5* enhanced HS tolerance in transgenic *Arabidopsis*.

75 To date, cystatin family genes had been well described in several plant species such as
76 *Arabidopsis*, rice, soybean, wheat, *Populus trichocarpa*, and *Brachypodium distachyon*
77 (Martinez and Diaz, 2008; Wang et al. 2015; Yuan et al. 2016; Dutt et al. 2016; Subburaj et al.
78 2017). However, a genome-wide study of cystatin family genes in Sorghum has not yet been
79 performed. Sorghum is the world's fifth biggest crop (after rice, wheat, maize, and barley),
80 belonging to a C4 grass that grows in arid and semi-arid regions (Taylor et al. 2010). Its drought
81 tolerance is a consequence of morphological and anatomical characteristics (i.e., thick leaf wax,
82 deep root system) and physiological responses (i.e., stay-green, osmotic adjustment). Hence,
83 Sorghum is an excellent model plant for the study of plant response to drought stress (Sunita et al.
84 2011). Recently, the completion of the whole genome assembly of Sorghum (*Sorghum bicolor* L.
85 Moench) makes it possible to identify and analyze cystatin family genes in Sorghum (Paterson et
86 al. 2009). In this study, we aimed to perform a genome-wide identification of *SbCys* family
87 genes in Sorghum and analyze their phylogeny, conserved motifs, structure, *cis*-elements, and
88 expression profile in different tissues. We also explored the expression patterns of *SbCys* genes
89 in response to biotic and abiotic stresses. The results may lay a foundation for further functional
90 analyses of cystatin genes.

91

92 MATERIALS AND METHODS

93 Identification of SbCys family members in Sorghum genome

94 The identification of SbCys candidates was conducted according to the methods of Lozano et al.
95 (2015) with some modification. The cystatin sequences of *Arabidopsis*, rice (*Oryza sativa*), and
96 barely (*Hordeum vulgare*) were downloaded from TAIR (<http://www.Arabidopsis.org>), the Rice
97 Genome Annotation Project (<http://rice.plantbiology.msu.edu/index.shtml>), and Ensembl
98 database (http://plants.ensembl.org/Hordeum_vulgare/Info/Index), respectively. The whole-
99 genome sequence of Sorghum was downloaded from Ensembl database
100 (http://plants.ensembl.org/Sorghum_bicolor/Info/Index). Then predicted proteins from the
101 Sorghum genome were scanned using HMMER v3 (<http://hmmer.org/>) using the Hidden Markov
102 Model (HMM) profile of cystatin (PF00031) from the Pfam protein family database
103 (<http://pfam.xfam.org/>) (Finn et al. 2011). From the proteins obtained using the raw cystatin
104 HMM, a high-quality protein set with a cut-off e -value $< 1 \times 10^{-10}$ was aligned and used to
105 construct a Sorghum specific cystatin HMM using hmmbuild from the HMMER v3 suite. Then
106 all proteins with e -value < 0.01 were selected by the new Sorghum specific HMM. Cystatin
107 sequences were further filtered based on the closest homolog from *Arabidopsis*, *Oryza sativa*,
108 and *Hordeum vulgare* using ClustalW and the UNIREF100 sequence database. Proteins that
109 have no typical domain (Aspartic acid proteinase inhibitor) and reactive site motif (QxVxG)
110 were removed from posterior analysis.

111 Sequence alignment, structure analysis, and phylogenetic tree construction

112 The Multiple Expectation for Motif Elicitation (MEME) program was used to identify conserved
113 motifs shared among SbCys proteins. The parameters of MEME were as follows: maximum
114 number of motifs, 10; optimum width, between 6 and 50; and number of repetitions, any.

115 The three-dimensional structures of Sorghum cystatins were modelled by the automated SWISS-
116 MODEL program (<http://swissmodel.expasy.org/interactive>). The known crystal structure of rice
117 oryzacystatin I (OC-I) and SiCYS (Hu et al. 2015; Yuan et al. 2016) were used to construct the
118 homology-based models. Structure analysis was conducted by the RasMol 2.7 program.

119 A phylogenetic tree was constructed using MEGA X with the maximum likelihood method
120 according to the Whelan and Goldman + freq. Model. Bootstrap analysis was performed by 1000
121 replicates with the p-distance model. The phylogenetic tree was visualized and optimized in
122 Figtree (<http://tree.bio.ed.ac.uk/software/figtree/>).

123 **Transcript structures, chromosomal location and gene duplication**

124 The genomic structure of each *SbCys* gene was derived from the alignment of their coding
125 sequence to their corresponding genome full-length sequence. The diagrams of these *SbCys*
126 genes were drawn by the Gene Structure Display Server (GSDS, <http://gsds.cbi.-pku.edu.cn/>)
127 (Hu et al. 2014). The chromosomal locations of *SbCys* genes were retrieved from the
128 Sorghum_bicolor_NCBIv3 map. The genes were plotted on chromosomes using the Map
129 Gene2chromosome (MG2C, version 2.0) tool (<http://mg2c.iask.in/>). Gene duplication events of
130 *SbCys* family genes were investigated according to the following two criteria: (1) the alignment
131 covered > 75% of the longer gene, (2) the aligned region had an identity > 75%, (3) located in
132 less than 100 kb single region or separated by less than five genes. For microsynteny analysis,
133 the CDS sequence of every cystatin from *Arabidopsis*, barley, rice, and Sorghum was used as the
134 query to search against all other cystatins using NCBI_blast software with $e\text{-value} \leq 1e^{-10}$. The
135 Circos software was used to display the results of collinear gene pairs (Krzywinski et al. 2009).

136 **Calculation of Ka and Ks**

137 To assess the degree of natural selection on *SbCys* genes, the rate ratio of *Ka* (nonsynonymous

138 substitution rate) to K_s (synonymous substitution rate) was calculated using KaKs Calculator 2.0
139 (Zhang et al. 2006). The K_a/K_s ratio > 1 , < 1 , or $= 1$ indicates positive, negative, or neutral
140 evolution, respectively (Yadav et al. 2015).

141 **Promoter analysis of *SbCys* genes**

142 To investigate the *cis*-regulatory elements in a promoter region, the upstream sequences (1.5 kb)
143 of the start codon in each *SbCys* gene were scanned in the PlantCARE database
144 (<http://bioinformatics.psb.ugent.be/webtools/plantcare/html/>) and New PLACE
145 (<https://www.dna.affrc.go.jp/PLACE/?action=newplace>).

146 **Analysis of interaction networks of the *SbCys* proteins**

147 The functional interacting network models of *SbCys* proteins were integrated using the web
148 STRING program (<http://string-db.org/>) based on an *Arabidopsis* association model; the
149 confidence parameters were set at a 0.40 threshold, the number of interactors was set to five
150 interactors. *Arabidopsis* AtCys proteins were mapped to Sorghum *SbCys* proteins based on their
151 homologous relationship. The interaction network of *SbCys* proteins was drawn by
152 Cytoscape_v3.6.0.

153 **Expression analysis of *SbCys* genes under biotic stresses**

154 The RNA-Seq data used for investigating the expression patterns of *SbCys* genes in various
155 tissues were downloaded from the NCBI SRA (Sequence Read Archive) database (ERP024508)
156 (Wang et al. 2018). Root, shoot, and seedling were collected at 14 days after germination.
157 Embryo, endosperm, and pericarp were collected at 20 days after pollination. Pollen samples
158 were collected at booting stage. Inflorescences were collected according to the sizes: 1-5 mm, 5-
159 10 mm, and 1-2 cm. Three biological replicates were performed for each plant tissue. RNA was
160 sequenced using the Illumina HiSeq 2500 system to generate 250 bp pair-end reads.

161 RNA-seq data of biotic stresses were obtained from two experiments. The first experiment
162 measured the transcriptome response of a resistant Sorghum (*Sorghum bicolor* L. Moench)
163 infected with *Bipolaris sorghicola* (Yazawa et al. 2013). RNA samples were collected at 0, 12,
164 and 24 hours post-inoculation with one biological replicate. RNA-seq was run using Illumina
165 technology to give 100-base-pair single-end reads on a HiSeq2000 system. The second study
166 measured changes in the transcriptome of Sorghum leaves infested by sugarcane aphid (Tetreault
167 et al. 2019). The RNA-seq data were downloaded from the NCBI SRA database. In this study,
168 two treatments (infested and control) were arranged and two Sorghum genotypes (resistant
169 cultivar RTx2783 and susceptible cultivar BCK60) were used. Leaf samples were collected from
170 treated and control plants at 5, 10, and 15 days post sugarcane aphid infestation. Three biological
171 replicates were performed for all treatment and time combinations. RNA was sequenced using
172 the Illumina Hiseq 2500 platform to generate 100 bp single end reads. The accession numbers
173 and sample information were listed in Table S1. The differential expression of *SbCys* genes were
174 investigated by Hisat2 (<http://kim-lab.org/>), Htseq (<http://www.htseq.org/>), and DESeq2 (R
175 package) based on the RNA-seq data (Wen, 2017). The $p \leq 0.05$ and $|\logFC| \geq 1.5$ were set as the
176 cut-off criterion.

177 **Plant materials and treatments**

178 Seed of Sorghum (*Sorghum bicolor* L. cv. Jinza 35) were surface sterilized (15 min in 4%
179 NaClO), washed with distilled water several times, and transferred to moist germination paper
180 for 3 days in an incubator at 25 °C. These seedlings were grown in holes of foam floating plastic
181 containers (30 seedlings per container) with constant aeration in Hoagland solution in a growth
182 room with 14 h/30 °C light and 10 h/22 °C dark regime. The nutrient solution was routinely
183 changed every 3 days. At the three-leaf stage (the juvenile phase (Hashimoto et al. 2019)),

184 abiotic stresses including ABA, salinity, and dehydration treatments were initiated according to
185 the procedures described in previous reports (Dugas et al. 2011; Wang et al. 2012; Yan et al.
186 2017). The plants were transferred quickly to the nutrient solution containing 0.1 mM ABA
187 (dissolved in ethanol), 5 μ L ethanol (control for ABA treatment), 250 mM sodium chloride
188 (NaCl), or 15% (W/V) polyethylene glycol (PEG) 6,000. The central part of flag leaves from
189 randomly selected Sorghum plants were harvested respectively at 0, 12, and 24 hours post-
190 treatment per trial, and immediately frozen in liquid nitrogen and then stored at -80°C prior to
191 RNA isolation. For each treatment at a given time, three biological replicates were used. The leaf
192 samples of 10 plants came from the same container for one biological replicate. That is, three
193 containers were used for three biological replicates respectively.

194 **RNA extraction and qRT-PCR analysis**

195 Total RNA of 100 mg leaf samples was isolated using the “TaKaRa MiniBEST Plant RNA
196 Extraction” Kit (TaKaRa, Dalian, China) following the manufacturer’s instructions. Purity and
197 concentration of RNA samples were evaluated by measuring the A_{260}/A_{230} and A_{260}/A_{280} ratios.
198 In order to digest the genomic DNA, the RNAs were treated with RNase-free DNase I. Reverse
199 transcription was performed according to the kit instructions (Promega, Madison, USA). Primer
200 pairs for qRT-PCR analysis were designed by Primer3Plus program
201 (<http://www.bioinformatics.nl>), and were shown in Table S2. A 20 μ l reaction volume containing
202 0.4 μ l of each primer (forward and reverse), 2 μ l 10-fold diluted cDNA, 7.2 μ l of nuclease-free
203 water, and 10 μ l of GoTaq® qPCR Master Mix (Perfect Real Time; Promega). PCR reaction
204 included one cycle at 95°C for 3 min, followed by 39 cycles of 95°C for 15 s, 60°C for 30s, and
205 72°C for 20s. The reactions were conducted using the CFX96 Real-Time PCR Detection System
206 (Bio-Rad Laboratories, Inc.). Three independent biological replicates and two technical

207 replicates of each sample were performed. Gene-specific amplification of both reference and
208 *cystatin* genes were standardized by the presence of a single, dominant peak in the qRT-PCR
209 dissociation curve analyses. All data were analyzed by CFX Manager Software (Bio-Rad
210 Laboratories, Inc.). The efficiency range of the qRT-PCR amplifications for all of the genes
211 tested was between 91% and 100%. The average target (*SbCys*) cT (threshold cycle) values were
212 normalized to reference (*β-actin*) cT values. The fold change between treated sample and control
213 was calculated using the slightly modified $2^{-(\Delta\Delta Ct)}$ method as described by Kebrom et al. (2010).
214 A probability of $p \leq 0.05$ was considered to be significant.

215

216 RESULTS

217 Identification and analysis of *SbCys* genes

218 To extensively identify all of *SbCys* family members in Sorghum, we constructed a Sorghum-
219 specific HMM for the *SbCys* domain to scan the Sorghum genome, and 22 gene candidates were
220 identified. After removing the repetitive and/or incomplete sequences, the rest of *SbCys*
221 sequences were submitted to Pfam (<http://pfam.xfam.org/>) and SMART ([http://smart.embl-
222 heidelberg.de/](http://smart.embl-heidelberg.de/)) to confirm the conserved domain. Finally, a total of 18 non-redundant *SbCys*
223 proteins were identified and were serially renamed from *SbCys1* to *SbCys17* according to their
224 location and order in chromosomes. Gene names, gene IDs, chromosomal locations, amino acid
225 numbers, protein sequences, and annotations assigned to GO terms of the identified *SbCys*
226 proteins were listed in Table S3. The average length of these *SbCys* proteins was 148 amino acid
227 residues and the length mainly centered on the range of 105 to 240 amino acid residues.
228 Chromosome distribution analysis showed that the number of *SbCys* genes on each chromosome
229 is different (Fig. 1). Chromosome 1 had the greatest number of *SbCys* genes (9 genes), followed

230 by chromosomes 9 and 3 (4 and 3 genes, respectively). Chromosomes 2 and 4 had just one
231 *SbCys* gene, whereas chromosomes 5, 6, 7, 8, and 10 had no *SbCys* genes.

232 **Gene structure analysis of *SbCys* genes**

233 The analysis of exon-intron structure can provide useful information about the gene function,
234 organization, and evolution of multiple gene families (Xu et al. 2012). Schematic structures of
235 *SbCys* genes from Sorghum were obtained using the GSDS program (Fig. 2). Among the *SbCys*
236 genes, more than half (12, 66.7%) were intronless, three genes (*SbCys11*, *SbCys15*, and *SbCys16*)
237 had one intron, two genes (*SbCys14* and *SbCys17*) had two introns, and one gene (*SbCys10*) had
238 three introns. These six *SbCys* genes with one or more introns were clustered into one clade,
239 suggesting the evolutionary event may affect the gene structure (Altenhoff et al. 2012).

240 **Sequence alignment, protein motifs analysis, and structural predication of *SbCys***

241 Alignments of *SbCys* sequences were carried out to search for amino acid variants that could
242 lead to differences in their inhibitory capability for cysteine proteases. The results were shown in
243 Fig. 3a. N-terminal and C-terminal extensions with varying lengths that presented in several
244 *SbCys* proteins were not displayed in the comparison. These predicted structures shared many
245 identical residues including α -helix and the four β -sheets (β 2-5) (Fig. 3a). Analysis of conserved
246 motifs of *SbCys* proteins also revealed that some typical conserved motifs could be detected in
247 most *SbCys* proteins, such as motif 1, 2, 3, and 4. These motifs formed a fundamental structural
248 combination (Fig. 3b and 3c). Motif 1 was conserved in the central loop region with a consensus
249 sequence of “QxVxG” and could be detected in most *SbCys* proteins, which played an important
250 role in the inhibitory capacity of cystatins towards their target cysteine proteases (Meriem et al.
251 2010). Motif 2 contained a particular consensus sequence ([LVI][GA][RQG][WF]AV) that
252 conformed to a predicted secondary α -helix structure (Martinez et al. 2009). The other two

253 typical motifs for SbCys proteins, motif 3 (V[WY][EVG]KPW) and motif 4 ([RK]xLxxF),
254 which were firstly described in tobacco (Zhao et al. 2014), were also detected in most SbCys
255 proteins, indicating their conserved and common role in both dicots and monocots. Motif 5
256 existed only in 3 SbCys family members (SbCys5, SbCys8, and SbCys15). Details of the 5
257 conserved motifs were shown in Fig. S1.

258 The predicted three-dimensional structures of the Sorghum cystatins were established using the
259 SWISS-MODEL program based on the known crystal structure of OC-I and SiCYS (Fig. 4).
260 Although these structures were predicted with variable degrees of accuracy, all of Sorghum
261 cystatins shared similar protein structure with rice OC-I (Fig. 4a), excepting SbCys10 that shared
262 similar protein structure with SiCYS (Fig. 4b). In addition, SbCys14 showed a significant
263 variation in its predicted three-dimensional structures, might due to an extra α -helix that existed
264 in the C-terminal extension of SbCys14. Two important motifs (the conserve QxVxG motif and
265 W residue) of Sorghum cystatins involved in the interaction with the target cysteine enzymes
266 were also shown in Fig. 4. The predicted structure of SbCys13 showed some distortions in the
267 region of the β 2 sheet, probably due to the insertion of a methionine in the first position of the
268 conserved QxVxG motif.

269 **Phylogenetic analysis of *SbCys* genes**

270 The cystatin gene family is highly conserved in both monocots and dicotyledons (Martinez and
271 Diaz, 2008). To investigate the phylogenic relationships of SbCys proteins to other known plant
272 cystatins, a multiple sequence alignment of SbCys sequences to the sequences from *Arabidopsis*,
273 rice, and barley was conducted by the ClustalW program. As showed in Fig. 5, these cystatins
274 were categorized into three groups, including Group I, Group II, and Group III. A total of 21
275 cystatins were classified to Group I and 6 cystatins from Sorghum. Group II contained 7

276 cystatins, only one cystatin from Sorghum. The remaining 21 proteins were assigned to Group III
277 and 11 *SbCys* proteins fell into this group. In addition, some bootstrap values in the phylogenetic
278 tree were low, suggesting that high sequence differentiation in these cystatins occurred.
279 Microsynteny analysis indicated that one orthologous gene pair was identified in the cross of
280 barley and Sorghum, rice and Sorghum, respectively, while no orthologous gene pair between
281 *Arabidopsis* and Sorghum was found (Fig. S2). These data indicated that *SbCys* genes were more
282 closely related to rice and barley than *Arabidopsis*. Interestingly, a pair of *SbCys* genes (*SbCys2-*
283 *1* and *SbCys2-2*) was involved in the tandem duplication event in Sorghum (Fig. S2). Analysis of
284 duplicated *SbCys* genes showed that the *Ka/Ks* ratio far less than 1, varying from 0.0976 to
285 0.5679 (Table S4), indicating that negative selection occurred in the duplication event.

286 **Promoter analysis of *SbCys* genes**

287 In order to obtain useful information on the regulatory mechanism of cystatin gene expression,
288 the 1.5 kb upstream sequences from the translation start sites of *SbCys* genes were submitted into
289 PlantCARE database to detect the *cis*-elements. Various putative plant regulatory elements in the
290 promoter region of *SbCys* genes were shown in Fig. 6 and Table S5. Several potential regulatory
291 elements involved in stress-related transcription factor-binding sites were found, including G-
292 box, W-box, TC-rich repeats, MBS, heat shock elements (HSEs), and ABA-response element
293 (ABRE). The identified *SbCys* genes possessed at least 1 stress-response-related *cis*-element,
294 suggesting that the expressions of *SbCys* genes were related to the biotic and abiotic stresses. All
295 of *SbCys* genes had one or more G-box with the exception of *SbCys9*, implying that these *SbCys*
296 genes could be induced by light stress. 14 *SbCys* genes possessed MBS element, ABRE element
297 was found in 12 *SbCys* genes, HSE element was located in 10 *SbCys* genes, and TC-rich repeats
298 and W-boxes were located in 8 genes. In addition *Skn-1*_motif was conserved in the promoter

299 regions of most *SbCys* genes, indicating these genes were associated with the regulation of seed
300 storage protein gene expression (Strömvik and Fauteux, 2009). The high diversity of the *cis*-
301 acting elements suggested that these *SbCys* genes might have a wide range of functional roles
302 and could be involved in multiple stress responses and growth and development progress (Zhang
303 et al. 2008).

304 **Protein interaction network of *SbCys* proteins**

305 In this study, the interactions of the *SbCys* proteins were investigated in an *Arabidopsis*
306 association model using STRING software. As shown in Fig. 7, the interaction network of
307 cystatins showed a complex functional relationship. *AtCys2* (corresponding to *SbCys12*)
308 interacted with stress related proteins (*AT1G56280*, *AT3G19580*, *AT5G67450*, and *AtCys1*) and
309 growth and development related proteins (*AT1G63100* and *AT5G04340*), *AtCys1*
310 (corresponding to *SbCys11*, 15, 16, and 17) interacted with some vacuolar-processing enzyme
311 which involved in processing of vacuolar seed protein precursors into the mature forms, and
312 *AtCys5* (corresponding to *SbCys1*, 2-1, 3, 4, 5, 6, 7, 8, 9, and 13) interacted with several lipid-
313 transfer proteins (*AT1G07747*, *AT1G52415*, *AT2G16592*, *AT3G29152*, and *AT4G12825*). The
314 results suggested that cystatins might be associated with many biological processes by protein
315 interactions, such as pollen development, stress responses, and seed maturation (Wang et al.
316 2012).

317 **Expression profile of *SbCys* genes in different Sorghum tissues**

318 To obtain the spatial and temporal expression patterns of all *SbCys* genes, RNA-seq data
319 (ERP024508) were downloaded to explore the expression levels of *SbCys* genes in different
320 tissues including root, stem, seedling, pollen, endosperm, embryo, inflorescence (1-5mm, 1-
321 10mm, and 1-2cm), and pericarp. As shown in Fig. 8 and S3, most *SbCys* genes were expressed

322 in one tissue at least, except for *SbCys13*, which were barely expressed in any tissue. The
323 expression patterns of *SbCys* genes were significantly different between reproductive tissues and
324 vegetative tissues, such as *SbCys2-1*, *SbCys3*, *SbCys4*, *SbCys5*, *SbCys7*, *SbCys9*, *SbCys12*, and
325 *SbCys17*, which showed relatively higher expression levels in reproductive tissues including
326 pollen, endosperm, embryo, and pericarp than in vegetative tissues, while the expression of
327 *SbCys7* and *SbCys15* were higher in vegetative tissues than in reproductive tissues. It was worth
328 noting that the majority of *SbCys* genes had lower expression levels during inflorescence
329 development excepting *SbCys17* which displayed a higher expression pattern.

330 **Expression of *SbCys* genes under biotic stresses**

331 To gain insight into the potential roles of *SbCys* genes in response to *Bipolaris sorghicola*
332 infection and sugarcane aphid infestation, the relative expression patterns of these genes were
333 investigated by using the public transcription data from NCBI SRA database (DRP000986 and
334 SRP162227, respectively). As shown in Fig. 9 and 10, the expression patterns of *SbCys* genes
335 were different under the two biotic stresses. In response to *Bipolaris sorghicola* infection, seven
336 *SbCys* genes were induced and only 2 genes (*SbCys12* and *SbCys13*) were suppressed in the
337 infected Sorghum leaves compared with control (Fig. 9a). However, under aphid infestation, four
338 *SbCys* genes (*SbCys4*, *SbCys10*, *SbCys11*, and *SbCys14*) were up-regulated and 3 genes (*SbCys1*,
339 *SbCys3*, and *SbCys17*) were down-regulated relative to control in the susceptible Sorghum line
340 (BCK60). In the resistant Sorghum line (RTx2783), only two *SbCys* genes (*SbCys4* and *SbCys11*)
341 were induced, and the rest were barely expressed in Sorghum leaves with aphid infestation (Fig.
342 9b and 10). These results might suggest that *SbCys* genes played different roles in responding to
343 pathogen infection and aphid infestation.

344 **Expression profiling of *SbCys* genes under abiotic stresses**

345 We also investigated the expression of *SbCys* genes in response to various abiotic stresses
346 including dehydration, salt shock, and ABA (Fig. 11). Under dehydration stress, seven *SbCys*
347 genes (*SbCys4*, *SbCys5*, *SbCys6*, *SbCys9*, *SbCys10*, *SbCys11*, and *SbCys17*) were induced to
348 present a significant up-regulation from 0 to 24 h, while the expressions of *SbCys2-1*, *SbCys12*,
349 *SbCys15*, and *SbCys16* were decreased. Furthermore, the expressions of 4 *SbCys* genes (*SbCys1*,
350 *SbCys3*, *SbCys8*, and *SbCys14*) displayed an up-down trend from 0 h to 24 h (Fig. 11a). With salt
351 shock treatment, the expressions of *SbCys2-1*, *SbCys3*, *SbCys4*, *SbCys8*, *SbCys10*, and *SbCys11*
352 were significantly up-regulated at all treatment time points, whereas *SbCys16* showed a
353 significant down-regulated trend (Fig. 11b). In addition, *SbCys6*, *SbCys13*, *SbCys14*, *SbCys15*,
354 and *SbCys17* showed up-down expression trends, but *SbCys5* displayed a down-up expression
355 pattern (Fig. 11b). After exogenous ABA treatment, the expressions of 4 *SbCys* genes (*SbCys2-2*,
356 *SbCys3*, *SbCys4*, and *SbCys7*) were significantly up-regulated at three time points, but 9 genes
357 (*SbCys1*, *SbCys2-1*, *SbCys5*, *SbCys8*, *SbCys10*, *SbCys11*, *SbCys13*, *SbCys14*, and *SbCys17*) were
358 down-regulated. Additionally, *SbCys12*, *SbCys15*, and *SbCys16* displayed up-down expression
359 trends (Fig. 11c). Interestingly, all *SbCys* genes were up-regulated in response to one or two
360 stresses except *SbCys4* that was significantly induced under dehydration, salt, and ABA stresses,
361 suggesting that *SbCys4* might play an important role in response to different stress responses.

362

363 **DISCUSSION**

364 Plant cystatins are a group of intrinsic small proteins, whose members play important roles in
365 diverse biological processes and stress responses (Martinez et al. 2016; Meriem et al. 2010).
366 Recently, a large number of sequence data from different plant species have been uploaded in
367 GenBank, which provide convenience for us to describe their characteristics, and several

368 cystatins families have been identified from plants, such as rice, soybean, and wheat (Wang et al.
369 2015; Dutt et al. 2016; Yuan et al. 2016). However, little is known about the cystatin family in
370 Sorghum. In the present study, we identified 18 *SbCys* genes from the Sorghum genome. The
371 number was less than that of *B. distachyon* genome, where 25 *BdCys* members were identified
372 (Subburaj et al. 2017). The 18 members in Sorghum was a larger number than found in rice (11
373 genes) and *Arabidopsis* (7 genes) (Wang et al. 2015), but was similar to soybean (20 members)
374 (Yuan et al. 2016). The difference on the cystatin number might reflect the adaptation of plants
375 to environment.

376 The identified *SbCys* genes were unevenly distributed on chromosomes 1, 2, 3, 4, and 9, and half
377 of them were distributed on chromosome 1 (Fig. 1). The uneven distribution of *cystatin* genes in
378 chromosomes was also found in the *B. distachyon* genome and the *Oryza sativa* genome
379 (Subburaj et al. 2017; Wang et al. 2015). This phenomenon might be due to the tandem
380 duplication events of *cystatin* genes on the chromosomes (Li et al. 2017). Several tandem
381 duplication events occurred at chromosomes 1 of the *B. distachyon* genome (Subburaj et al.
382 2017). Two tandem duplication events (*OsCys4/OsCys5* and *OsCys6/OsCys7*) were found
383 among *OsCys* genes, and existed in chromosomes 1 and 3 (Wang et al. 2015). One tandem
384 duplication event (*SbCys2-1/SbCys2-2*) occurred at chromosome 1 of the Sorghum genome (Fig.
385 S2). Eighteen *SbCys* genes were divided into three groups based on phylogenetic analysis (Fig.
386 5). Some conserved motifs among *SbCys* proteins had been identified by the alignment of the
387 amino acid sequences (Fig. 3). However, the conservation was accompanied with the differences
388 in some important amino acids indicated that *SbCys* family members might undergo a complex
389 evolutionary history. The variation of crucial amino acids of cystatins might have a significant
390 influence on their respective functions (Tremblay et al. 2019). For example, the QxVxG motif

391 could directly enter and interact with the active site of targeted enzymes. The motif was
392 conserved in all *SbCys* proteins with the exceptions of 5 cystatins (*SbCys1*, *SbCys6*, *SbCys8*,
393 *SbCys9*, and *SbCys13*) that were partially modified by the insertion or variation in important
394 residues (Fig. 3a). Furthermore, three *SbCys* proteins (*SbCys8*, *SbCys9*, and *SbCys13*) showed
395 significant variations with other *Sorghum* cystatins in their predicted three-dimensional
396 structures (Fig. 4). The variations in vital amino acid residues might result in the change in
397 cystatin inhibitory action (Tremblay et al. 2019). In addition, two novel motifs, motif 3
398 (V[WY][EVG]KPW) and motif 4 ([RK]xLxxF), firstly described in tobacco (Zhao et al. 2014),
399 were also identified in the C-terminalin of many *SbCys* proteins. The contribution of the two
400 new motifs to cystatin inhibitory action needs to be further studied.

401 During past decades, plant cystatins were reported to play essential roles in inhibiting
402 endogenous and exogenous cysteine proteases activities during seed development (Tremblay et
403 al. 2019). In the present study, as revealed by RNA-seq data analysis (Fig. 8 and S3), the
404 expression levels of several *SbCys* family genes were higher in reproductive tissues than in
405 vegetative tissues, which were consistent with the reports that most cystatins were specifically
406 expressed in developing seeds and played a role in seed development (Dutt et al. 2010; Zhao et al.
407 2014). Moreover, promoter analysis showed that the highly expressed *SbCys* genes in
408 reproductive tissues possessed endosperm expression-related *cis*-elements (Skn-1 and
409 GCN4_motif) (Fig. 6 and Table S5). Our protein interaction prediction results also showed that
410 several *SbCys* proteins could interact with many functional proteins (e.g., growth and
411 development related proteins, vacuolar-processing enzyme, and lipid-transfer proteins) (Fig. 7),
412 implying these cystatins were involved in regulating the gene expression of cereal grain storage
413 proteins (Diaz-Mendoza et al. 2016).

414 Plant cystatins are involved in various biotic stress responses and probably act as defense
415 proteins against pest infestation and pathogen infection (Meriem et al. 2010). At present, some
416 cystatins with insecticidal activity have been isolated from many plants, such as barley, tomato,
417 and potato (Rasoolizadeh et al. 2017; Siddiqui et al. 2017; Velasco-Arroyo et al. 2018; Goulet et
418 al. 2020). Several cystatins having antifungal activities were also isolated from taro, cacao, and
419 wheat (Christova et al. 2018; Pirovani et al. 2010; Chen et al. 2014). Although studies on
420 insecticidal and antifungal activity of plant cystatins have been well established *in vitro*, the
421 knowledge about their roles in plants in response to biotic stresses is limited. To explore the
422 properties of *SbCys* genes responding to pest infestation and pathogen infection, we conducted
423 the analysis on the expression patterns of *SbCys* genes. The results showed that the expressions
424 of most *SbCys* genes were induced during *Bipolaris sorghicola* infection, suggesting these
425 cystatins played functions in inhibiting exogenous cysteine proteases secreted by pathogens to
426 infect plant tissues (Fig. 9a). Interestingly, for sugarcane arthropods infestation, only two genes
427 (*SbCys4* and *SbCys11*) were up-regulated significantly in susceptible and resistant Sorghum lines
428 (Fig. 9b and 10). These differential expression patterns between *SbCys* genes might suggest that
429 some of them had evolved to inhibit specific cysteine proteinases. The exact roles of these *SbCys*
430 genes in insecticidal and antifungal activity *in vivo* are worthy to be explored in further study.

431 *Cystatin* genes are also involved in various abiotic stress responses in plants. In *Arabidopsis*, the
432 expression levels of *AtCYS1* and *AtCYS2* were enhanced by high temperature and wounding
433 stresses (Hwang et al. 2010). *AtCYSa* and *AtCYSb* were also induced by different abiotic stresses,
434 e.g., salt, drought, oxidation, and cold stresses (Zhang et al. 2008). Velasco-Arroyo et al. (2018)
435 reported that the silence of barley *HvCPI-2* and *HvCPI-4* specifically modified leaf responses to
436 drought stress. Wang et al. (2015) observed the significant change in the expression levels of

437 several rice *OsCYS* genes under cold, drought, salt, and hormone treatments. In the present study,
438 most *SbCys* genes were found to have positive or negative responses to dehydration, salt, and
439 ABA stresses. Moreover, the interaction results showed that most cystatins could interact with
440 stresses-related proteins, implying that the cystatins played critical roles in response to diverse
441 stress conditions. Notably, the expression of *SbCys4* was significantly up-regulated under three
442 stress conditions (Fig. 11), suggesting a specific role of *SbCys4* in responding to various stress
443 conditions. Promoter analysis indicated that stress-related *cis*-elements were widespread in the
444 promoter region of these cystatin genes (Table S5), and *SbCys4* possessed plenty of stress-related
445 *cis*-elements, including G-box, ABRE, HSE, MBS, and TC-rich repeats. These results provide an
446 effective reference for the functional verification of the *SbCys* family genes under abiotic
447 stresses.

448

449 CONCLUSIONS

450 In the current study, we identified 18 *SbCys* family genes in the Sorghum genome through a
451 genome-wide survey. The chromosomal localization, conserved protein domain, gene structure,
452 phylogenetic relationship, as well as the interaction network of these *SbCys* genes was
453 systematically analyzed, revealing special characteristics of *SbCys* family genes in Sorghum. The
454 identified *SbCys* genes displayed an uneven distribution in Sorghum chromosomes. All *SbCys*
455 genes shared similar exon/intron organization and conserved motifs. Phylogenetic analysis
456 suggested that Sorghum cystatins had higher homology with monocotyledon than dicotyledon.
457 Furthermore, the variation of amino acids in Sorghum cystatin critical active sites suggested that
458 they might undergo a complex evolutionary process and possess structural and functional
459 divergence. The expression profiles of *SbCys* genes in different tissues indicated that most *SbCys*

460 genes were involved in plant growth and development. Changes in the expression of *SbCys*
461 genes under biotic and abiotic stresses indicated that many *SbCys* genes played important roles in
462 response to unfavorable growth conditions. It was worth noting that the expression of *SbCys4*
463 was significantly enhanced under biotic and abiotic stresses, suggesting its unique role in
464 mediating the response of Sorghum to adverse environmental conditions.

465

466 REFERENCES

467 **Altenhoff AM, Studer RA, Robinsonrechavi M, Dessimoz C. 2012.** Resolving the ortholog
468 conjecture: orthologs tend to be weakly, but significantly, more similar in function than
469 paralogs. *PLoS Computational Biology* **8(5):e1002514** DOI
470 10.1371/journal.pcbi.1002514.

471 **Belenghi B, Acconcia F, Trovato M, Perazzolli M, Bocedi A, Polticelli F, Ascenzi P,**
472 **Delledonne M. 2010.** AtCYS1, a cystatin from *Arabidopsis thaliana*, suppresses
473 hypersensitive cell death. *European Journal of Biochemistry* **270(12):2593-604** DOI
474 10.1046/j.1432-1033.2003.03630.x.

475 **Blanca VA, Mercedes DM, Andrea GS, Santamaria B, Estrella M, Miguel TB, Kumlehn G,**
476 **Martinez J, Diaz I. 2018.** Silencing barley cystatins *HvCPI-2* and *HvCPI-4* specifically
477 modifies leaf responses to drought stress. *Plant Cell Environment* **41:1776-1790** DOI
478 10.1111/pce.13178.

479 **Chen PJ, Senthilkumar R, Jane WN, He Y, Tian Z, Yeh KW. 2014.** Transplastomic
480 *Nicotiana benthamiana* plants expressing multiple defence genes encoding protease
481 inhibitors and chitinase display broad-spectrum resistance against insects, pathogens, and
482 abiotic stresses. *Plant Biotechnology Journal* **12(4):1-13** DOI 10.1111/pbi.12157.

- 483 **Christova PK, Christov NK, Mladenov PV, Imai R. 2018.** The wheat multidomain cystatin
484 TaMDC1 displays antifungal, antibacterial, and insecticidal activities in planta. *Plant Cell*
485 *Reports* **37**:923-932 DOI 10.1007/s00299-018-2279-4.
- 486 **Diaz-Mendoza M, Dominguez-Figueroa JD, Velasco-Arroyo B, Cambra I, Gonzalez-**
487 **Melendi P, Lopez-Gonzalvez A, Garcia A, Hensel G, Kumlehn J, Diaz I, Martinez**
488 **M. 2016.** HvPap-1 C1A protease and HvCPI-2 cystatin contribute to barley grain filling
489 and germination. *Plant Physiology* **170**:2511-2524. DOI 10.1104/pp.15.01944.
- 490 **Díazmendoza M, Velascoarroyo B, Gonzálezmelendi P, Martínez M, Díaz I. 2014.** C1A
491 cysteine protease-cystatin interactions in leaf senescence. *Journal of Experimental*
492 *Botany* **65(14)**:3825-33 DOI 10.1093/jxb/eru043.
- 493 **Dugas DV, Monaco MK, Olson A, Klein RR, Kumari S, Ware D, Klein PE. 2011.** Functional
494 annotation of the transcriptome of *Sorghum bicolor* in response to osmotic stress and
495 abscisic acid. *BMC Genomics* **12**:514 DOI 10.1186/1471-2164-12-514.
- 496 **Dutt S, Singh VK, Marla SS, Kumar A. 2010.** In silico analysis of sequential, structural, and
497 functional diversity of wheat cystatins and its implication in plant defense. *Genomics*
498 *Proteomics Bioinformatics* **8(1)**:42-56 DOI 10.1016/S1672-0229(10)60005-8.
- 499 **Finn RD, Clements J, Eddy SR. 2011.** HMMER web server: interactive sequence similarity
500 searching. *Nucleic Acids Research* **39**:29-37 DOI 10.1093/nar/gkr367.
- 501 **Goulet MC, Sainsbury F, Michaud D. 2020.** Cystatin activity-based protease profiling to select
502 protease inhibitors useful in plant protection. *Methods in Molecular Biology* **2139**:353-366
503 DOI 10.1007/978-1-0716-0528-8.
- 504 **Hashimoto S, Tezuka T, Yokoi S. 2019.** Morphological changes during juvenile-to-adult phase
505 transition in Sorghum. *Planta* **250**:1557-1566 DOI 10.1007/s00425-013-1895-z.

- 506 **Hu B, Jin J, Guo AY, Zhang H, Luo J, Gao G. 2014.** GSDS 2.0: an upgraded gene feature
507 visualization server. *Bioinformatics* **31(8)**:1296 DOI 10.1093/bioinformatics/btu817.
- 508 **Hu YJ, Irene D, Lo CJ, Cai YL, Tzen TC, Lin TH, Chyan CL. 2015.** Resonance assignments
509 and secondary structure of a phytocystatin from *Sesamum indicum*. *Biomolecular NMR*
510 *Assignments* **9**:309-311 DOI 10.1007/s12104-015-9598-y.
- 511 **Hwang JE, Hong JK, Lim CJ, Chen H, Je J, Yang KA, Kim DY, Choi YJ, Lee SY, Lim CO.**
512 **2010.** Distinct expression patterns of two *Arabidopsis* phytocystatin genes, AtCYS1 and
513 AtCYS2, during development and abiotic stresses. *Plant Cell Reports* **29**:905-915 DOI
514 10.1007/s00299-010-0876-y.
- 515 **Kebrom TH, Brutnell TP, Finlayson SA. 2010.** Suppression of sorghum axillary bud
516 outgrowth by shade, phyB and defoliation signalling pathways. *Plant Cell Environment*
517 **33(1)**:48-58 DOI 10.4161/psb.5.3.11186.
- 518 **Kiggundu A, Muchwezi J, Van C, Viljoen A, Vorster J, Schlüter U, Kunert K, Michaud D.**
519 **2010.** Deleterious effects of plant cystatins against the banana weevil *Cosmopolites*
520 *sordidus*. *Arch Insect Biochemistry Physiology* **73(2)**:87-105 DOI 10.1002/arch.20342.
- 521 **Kiyosaki T, Matsumoto I, Asakura T, Funaki J, Kuroda M, Misaka T, Arai S, Abe K. 2007.**
522 Gliadain, a gibberellin-inducible cysteine proteinase occurring in germinating seeds of
523 wheat, *Triticum aestivum* L., specifically digests gliadin and is regulated by intrinsic
524 cystatins. *FEBS Journal* **164**:470-477 DOI 10.1111/j.1742-4658.2007.05749.x.
- 525 **Krzywinski M, Schein J, Birol I, Connors J, Gascoyne R, Horsman D, Jones SJ, Marra MA.**
526 **2009.** Circos: an information aesthetic for comparative genomics. *Genome research*
527 **19(9)**:1639-1645 DOI 10.1101/gr.092759.109.
- 528 **Li J, Yang XW, Li YC, Niu JS, He DX. 2017.** Proteomic analysis of developing wheat grains

- 529 infected by powdery mildew (*Blumeria graminis* f.sp. *tritici*). *Journal of Plant*
530 *Physiology* **215**:140-153 DOI 10.1016/j.jplph.2017.06.003.
- 531 **Li SF, Su T, Cheng GQ, Wang BX, Li X, Deng CL, Gao WJ. 2017.** Chromosome evolution in
532 connection with repetitive sequences and epigenetics in plants. *Genes* **8**:290 DOI
533 10.3390/genes8100290.
- 534 **Lima AM, dos Reis SP, de Souza CR. 2015.** Phytocystatins and their potential to control plant
535 diseases caused by fungi. *Protein and Peptid Letters* **22**:104-111 DOI
536 10.2174/0929866521666140418101711.
- 537 **Lozano R, Hamblin MT, Prochnik S, Jannink JL. 2015.** Identification and distribution of the
538 NBS-LRR gene family in the Cassava genome. *BMC Genomics* **16(1)**:360 DOI
539 10.1186/s12864-015-1554-9.
- 540 **Martinez M, Cambra I, Carrillo L, Diazmendoza M, Diaz I. 2009.** Characterization of the
541 entire cystatin gene family in barley and their target cathepsin L-like cysteine-proteases,
542 partners in the hordein mobilization during seed germination. *Plant Physiology*
543 **151(3)**:1531-1545 DOI 10.1104/pp.109.146019.
- 544 **Martinez M, Diazmendoza M, Carrillo L, Diaz I. 2007.** Carboxy terminal extended
545 phytocystatins are bifunctional inhibitors of papain and legumain cysteine proteinases.
546 *FEBS Letters* **581(16)**:2914-2918 DOI 10.1016/j.febslet.2007.05.042.
- 547 **Martinez M, Diaz I. 2008.** The origin and evolution of plant cystatins and their target cysteine
548 proteinases indicate a complex functional relationship. *BMC Evolutionary Biology*
549 **8(1)**:198-210 DOI 10.1186/1471-2148-8-198.
- 550 **Martinez M, Santamaria ME, Diazmendoza M, Arnaiz A, Carrillo L, Ortego F, Diaz I.**
551 **2016.** Phytocystatins: defense proteins against phytophagous insects and acari.

- 552 *International Journal of Molecular Sciences* **17(10)**:1747-1763 DOI
553 10.3390/ijms17101747.
- 554 **Meriem B, Urte S, Juan V, Marie-Claire G, Dominique M. 2010.** Plant cystatins. *Biochimie*
555 **92(11)**:1657-1666 DOI 10.1016/j.biochi.2010.06.006.
- 556 **Paterson AH, Bowers JE, Bruggmann R, Dubchak I, Grimwood J, Gundlach H, Haberer G,**
557 **Hellsten U, Mitros T, Poliakov A. 2009.** The *Sorghum bicolor* genome and the
558 diversification of grasses. *Nature* **457(7229)**:551-556 DOI 10.1038/nature07723.
- 559 **Pfaffl MW. 2001.** A new mathematical model for relative quantification in real-time RT-PCR.
560 *Nucleic Acids Research* **29**:e45 DOI 10.1093/nar/29.9.e45.
- 561 **Pirovani CP, Santiago AS, Santos LS, Micheli F, Margis R, Silva Gesteira R, Alvim FC,**
562 **Pereira GAG, Mattos JC. 2010.** *Theobroma cacao* cystatins impair *Moniliophthora*
563 *perniciosa* mycelial growth and are involved in postponing cell death symptoms. *Planta*
564 **232(6)**:1485-1497 DOI 10.2307/23391912.
- 565 **Rasoolizadeh A, Goulet MC, Guay JF, Cloutier C, Michaud D. 2017.** Population-associated
566 heterogeneity of the digestive Cys protease complement in Colorado potato beetle,
567 *Leptinotarsa decemlineata*. *Journal of Insect Physiology* **106**:125-133 DOI
568 10.1016/j.jinsphys.2017.03.001.
- 569 **Siddiqui AA, Khaki PS, Bano B. 2017.** Interaction of almond cystatin with pesticides:
570 Structural and functional analysis. *Journal Molecular Recognition* **30(3)**:e2586 DOI I
571 10.1002/jmr.2586.
- 572 **Song C, Kim T, Chung WS, Lim CO. 2017.** The *Arabidopsis* phytocystatin AtCYS5 enhances
573 seed germination and seedling growth under heat stress conditions. *Molecular Cells*
574 **40(8)**:577-586 DOI 10.14348/molcells.2017.0075.

- 575 **Strömvik MV, Fauteux F. 2009.** Seed storage protein gene promoters contain conserved DNA
576 motifs in *Brassicaceae*, *Fabaceae*, and *Poaceae*. *BMC Plant Biology* **9**:126 DOI
577 10.1186/1471-2229-9-126.
- 578 **Subburaj S, Zhu D, Li X, Hu Y, Yan Y. 2017.** Molecular characterization and expression
579 profiling of *Brachypodium distachyon* L. cystatin genes reveal high evolutionary
580 conservation and functional divergence in response to abiotic stress. *Frontiers in Plant*
581 *Science* **8**:743 DOI 10.3389/fpls.2017.00743.
- 582 **Sunita K, Klein RR, Andrew O, Monaco MK, Dugas DV, Doreen W, Klein PE. 2011.**
583 Functional annotation of the transcriptome of *Sorghum bicolor* in response to osmotic
584 stress and abscisic acid. *BMC Genomics* **12(1)**:514-514 DOI 10.1186/1471-2164-12-514.
- 585 **Tan Y, Yang Y, Li C, Liang B, Li M, Ma F. 2017.** Overexpression of *MpCYS4*, a phytocystatin
586 gene from *Malus prunifolia* (Willd.) Borkh., delays natural and stress-induced leaf
587 senescence in apple. *Plant Physiology Biochemistry* **115**:219-28 DOI
588 10.1016/j.plaphy.2017.03.025.
- 589 **Taylor SH, Hulme SP, Rees M, Ripley BS, Woodward FI, Osborne CP. 2010.**
590 Ecophysiological traits in C₃ and C₄ grasses: A phylogenetically controlled screening
591 experiment. *New Phytologist* **185(3)**:780-791 DOI 10.1111/j.1469-8137.2009.03102.x.
- 592 **Tetreault HM, Grover S, Scully ED, Gries T, Palmer N, Sarath G, Louis J, Sattler SE. 2019.**
593 Global responses of resistant and susceptible Sorghum (*Sorghum bicolor*) to sugarcane
594 aphid (*Melanaphis sacchari*). *Frontiers in Plant Science* **10**:145 DOI
595 10.3389/fpls.2019.00145.
- 596 **Tremblay J, Goulet MC, Michaud D. 2019.** Recombinant cystatins in plants. *Biochimie*
597 **166**:184-193 DOI 10.1016/j.biochi.2019.06.006.

- 598 **Valdes-Rodriguez S, Galvan-Ramirez JP, Guerrero-Rangel A, Cedro-Tanda A. 2015.**
599 Multifunctional amaranth cystatin inhibits endogenous and digestive insect cysteine
600 endopeptidases: A potential tool to prevent proteolysis and for the control of insect pests.
601 *Biotechnology Applied Biochemistry* **62**:634-641 DOI 10.1002/bab.1313.
- 602 **Velasco-Arroyo B, Diaz-Mendoza M, Gomez-Sanchez A, Moreno-Garcia B, Santamaria**
603 **ME, Torija-Bonilla M, Hensel G, Kumlehn J, Martinez M, Diaz I 2018.** Silencing
604 barley cystatins HvCPI-2 and HvCPI-4 specifically modifies leaf responses to drought
605 stress. *Plant Cell and Environment* **41(8)**:1776-1790 DOI 10.1111/pce.13178.
- 606 **Wang B, Regulsk M, Tseng E, Olson A, Goodwin S, McCombie WR, Ware D. 2018.** A
607 comparative transcriptional landscape of maize and Sorghum obtained by single-
608 molecule sequencing. *Genome Research* **28(6)**:921-928 DOI 10.1101/gr.227462.117.
- 609 **Wang HW, Hwang SG, Karuppanapandian T, Liu AH, Kim W, Jang CS. 2012.** Insight into
610 the molecular evolution of non-specific lipid transfer proteins via comparative analysis
611 between rice and sorghum. *DNA Research* **19**:179-194 DOI 10.1093/dnares/dss003.
- 612 **Wang W, Zhao P, Zhou XM, Xiong HX, Sun MX. 2015.** Genome-wide identification and
613 characterization of cystatin family genes in rice (*Oryza sativa* L.). *Plant Cell Reports*
614 **34(9)**:1579-1592 DOI 10.1007/s00299-015-1810-0.
- 615 **Wen G. 2017.** A simple process of RNA-Sequence analyses by Hisat2, Htseq, and DESeq2.
616 *International Conference Pp*:11-15 DOI 10.1145/3143344.3143354.
- 617 **Xu G, Guo C, Shan H, Kong H. 2012.** Divergence of duplicate genes in exon-intron structure.
618 *PNAS* **109(4)**:1187-1192 DOI 10.1073/pnas.1109047109.
- 619 **Yadav CB, Bonthala VS, Muthamilarasan M, Pandey G, Khan Y, Prasad M. 2015.**
620 Genome-wide development of transposable elements-based markers in foxtail millet and

- 621 construction of an integrated database. *DNA Research* **22**:79-90 DOI
622 10.1093/dnares/dsu039.
- 623 **Yan S, Li SJ, Zhai GW, Lu P, Deng H, Zhu S, Huang RL, Shao JF, Tao YZ, Zou GH. 2017.**
624 Molecular cloning and expression analysis of duplicated polyphenol oxidase genes reveal
625 their functional differentiations in Sorghum. *Plant Science* **263**:23-30 DOI
626 10.1016/j.plantsci.2017.07.002.
- 627 **Yazawa T, Kawahigashi H, Matsumoto T, Mizuno H. 2013.** Simultaneous transcriptome
628 analysis of Sorghum and *Bipolaris sorghicola* by using RNA-seq in combination with *De*
629 *novo* transcriptome assembly. *PLoS One* **8(4)**:e62460 DOI
630 10.1371/journal.pone.0062460.
- 631 **Yuan S, Li R, Wang L, Chen H, Zhang C, Chen L, Hao Q, Shan Z, Zhang X, Chen S. 2016.**
632 Search for nodulation and nodule development-related cystatin genes in the genome of
633 soybean (*Glycine max*). *Frontiers in Plant Science* **7**:1595 DOI 10.3389/fpls.2016.01595.
- 634 **Zhang X, Liu S, Takano T. 2008.** Two cysteine proteinase inhibitors from *Arabidopsis thaliana*,
635 AtCYSa and AtCYSb, increasing the salt, drought, oxidation, and cold tolerance. *Plant*
636 *Molecular Biology* **68**:131-143 DOI 10.1007/s11103-008-9357-x.
- 637 **Zhao P, Zhou XM, Zou J, Wang W, Wang L, Peng XB, Sun MX. 2014.** Comprehensive
638 analysis of cystatin family genes suggests their putative functions in sexual reproduction,
639 embryogenesis, and seed formation. *Journal of Experimental Botany* **65(17)**:5093-5108
640 DOI 10.1093/jxb/eru274.
- 641 **Zhang Z, Li J, Zhao XQ, Wang J, Wong GK, Yu J. 2006.** KaKs_Calculator 2.0: Calculating
642 Ka and Ks through model selection and model averaging. *Genomics Proteomics*
643 *Bioinformatics* **4(4)**:259-263 DOI 10.1016/S1672-0229(10)60008-3.

644

645

646

647

Figure 1

Chromosome localization of *SbCys* genes.

Chromosome number is indicated at the top of each bar. The size of chromosome was labeled on the left of the figure.

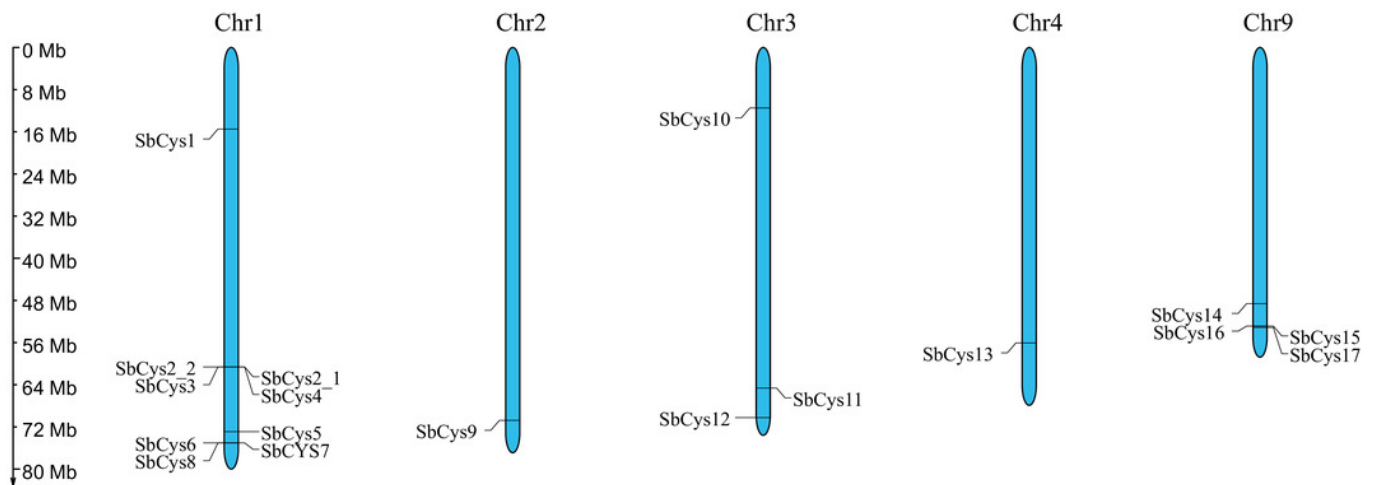


Figure 2

Phylogenetic relationship and gene structure of *SbCys* genes.

A phylogenetic tree was constructed using MEGA X by the maximum likelihood method with 1000 bootstrap replicates. Exon/intron structures were identified by online tool GSDS.

Lengths of exons and introns of each *SbCys* genes were exhibited proportionally. Exons and introns are shown by blue bars and black horizontal lines, respectively.

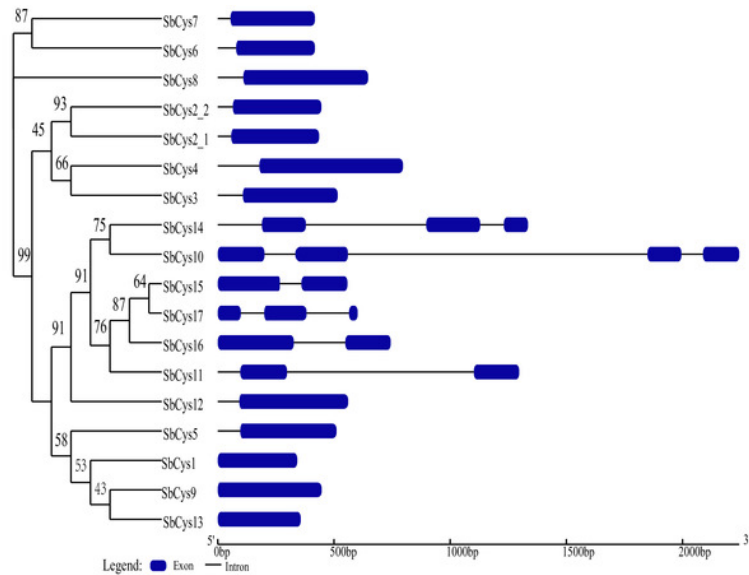


Figure 3

The amino acid alignment and conserved motifs distribution of SbCys.

(A) The locations of the secondary structures (α -helix and β -sheets) were included. The main cystatin conserved motifs are in black boxes. The strong and weak conservative changes in amino acids are marked by dark gray and light gray font, respectively. (B) The motifs were identified by MEME. Each motif was represented by one color box. (C) Conserved protein motif 1 (QxVxG), motif 2 (LARFAV and G-residue), motif 3 (W-residue), motif 4 ([RK]xLxxF), and motif 5 (P-residue) presented in the variable region of cystatin genes.

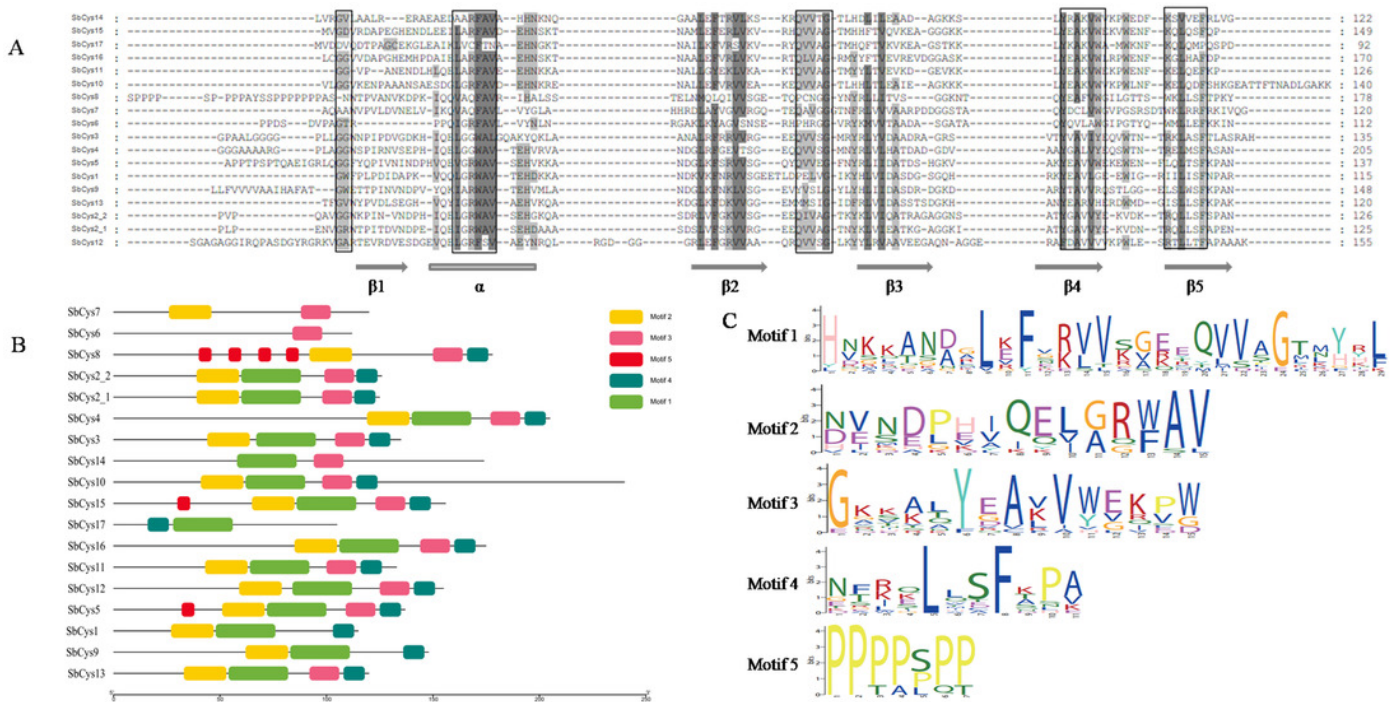


Figure 4

The three-dimensional structure prediction of Sorghum cystatins.

(A) The three-dimensional structures of SbCys proteins were predicted using the automated SWISS-MODEL program with OC-I as a template. (B) The three-dimensional structure of SbCys10 was predicted using the automated SWISS-MODEL program with SiCYS as a template. Two important motifs involved in the interaction with the target enzymes are indicated: the reactive site (asterisks) and W residue (crosses).

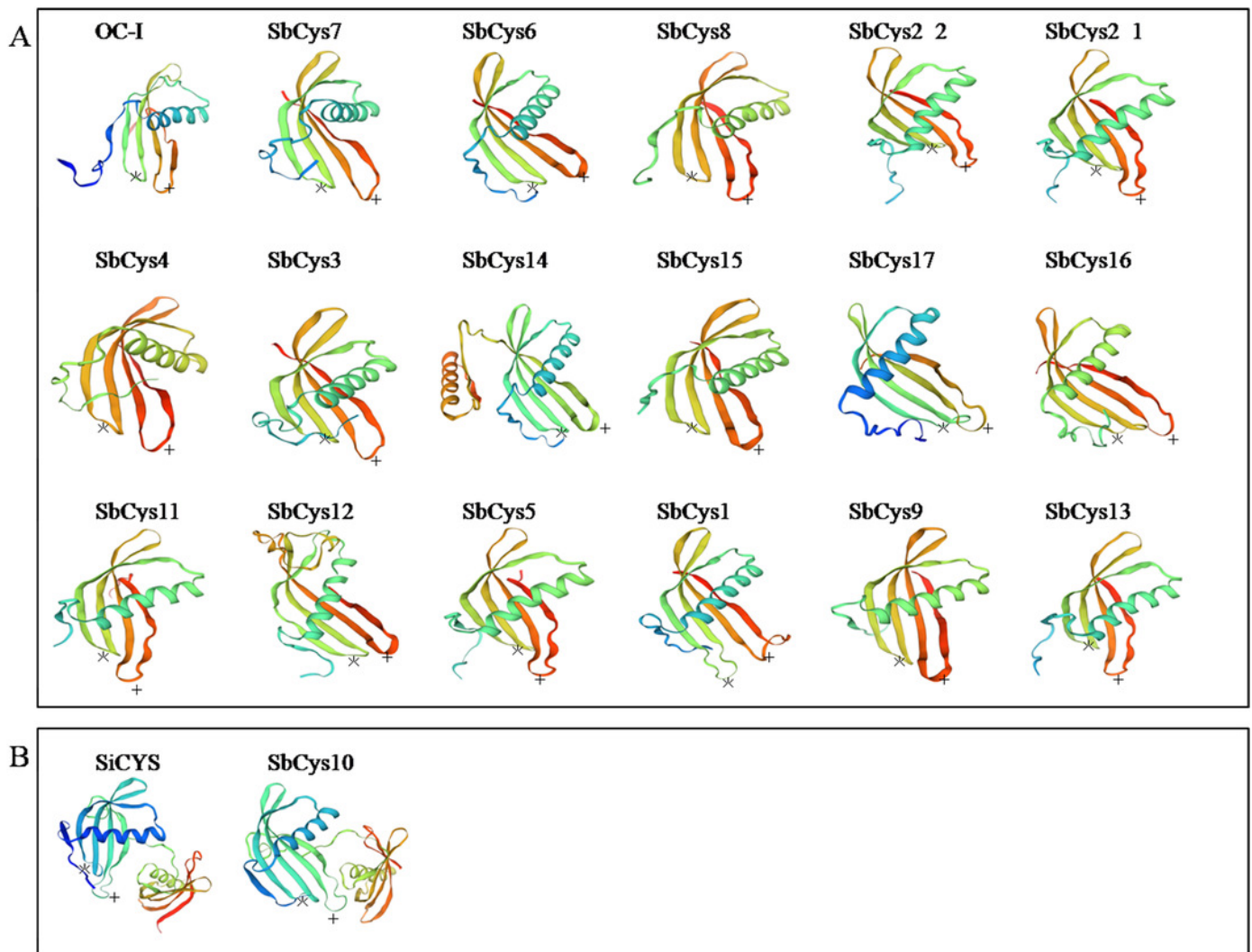


Figure 5

Phylogenetic relationships of the cystatins from *Arabidopsis*, rice, barley and Sorghum.

The phylogenetic tree was constructed by MEGA X with the maximum likelihood method. The numbers at the nodes indicate the bootstrap values. Gene names with black, red, and blue represented Group I, Group II, and Group III, respectively.

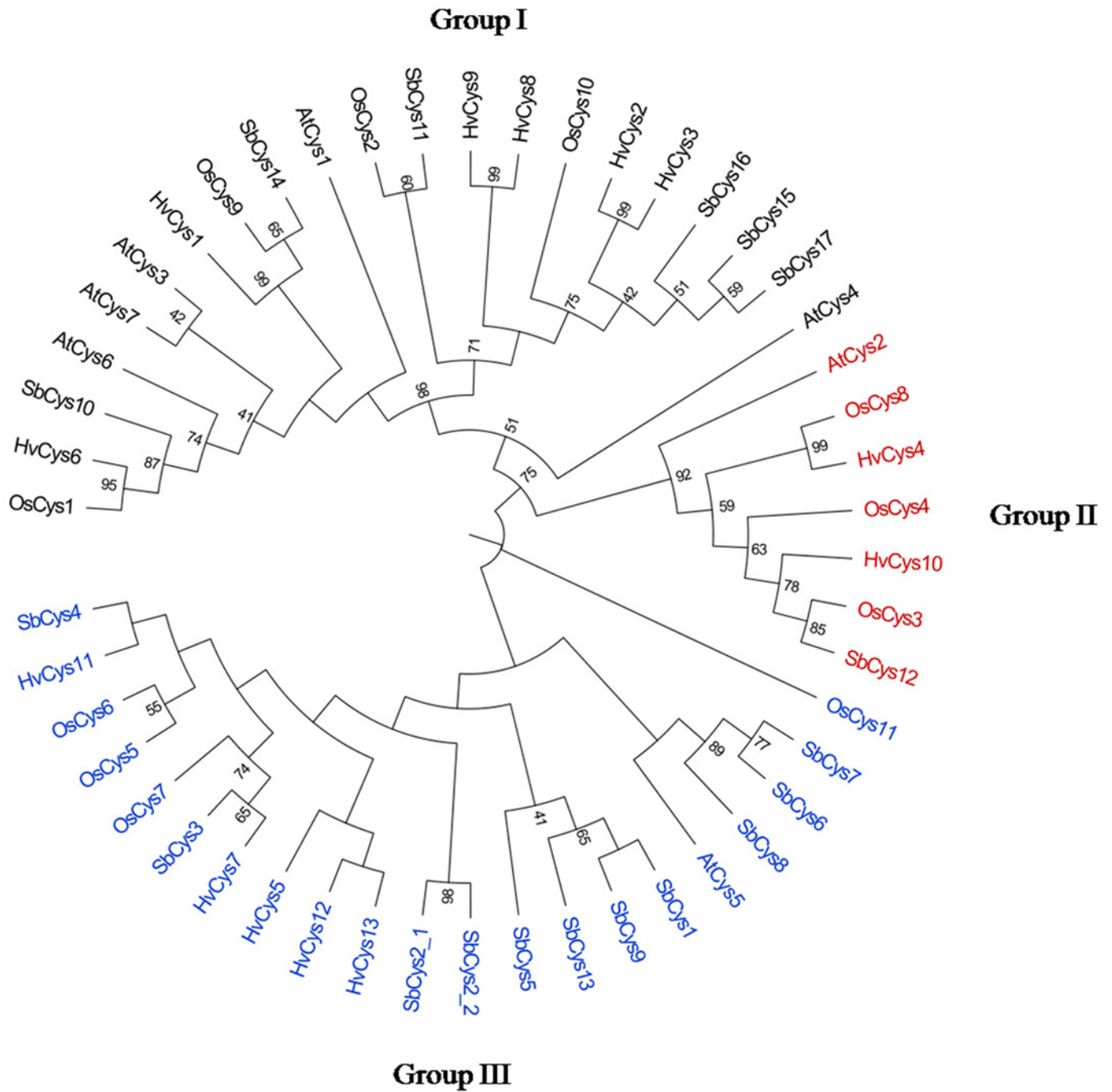


Figure 6

The distribution of *cis*-elements in the 1.5 kb upstream promoter regions of *SbCys* genes.

The *cis*-elements in the promoter region of *SbCys* genes were predicted using PlantCARE database (<http://bioinformatics.psb.ugent.be/webtools/plantcare/html/>). Different *cis*-elements were represented by different shapes and colors.

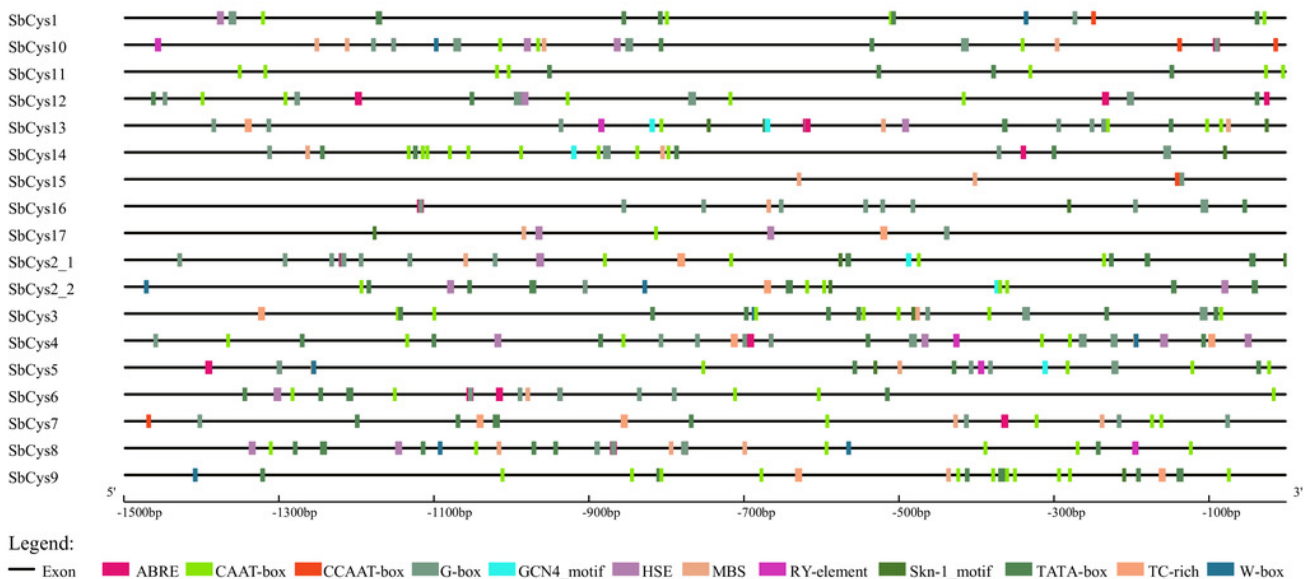


Figure 7

The interaction networks of SbCys proteins according to the orthologs in *Arabidopsis*.

Functional interacting network models were integrated using the STRING tool, and the confidence parameters were set at a 0.40 threshold. Homologous genes in Sorghum and *Arabidopsis* are shown in black and red, respectively.

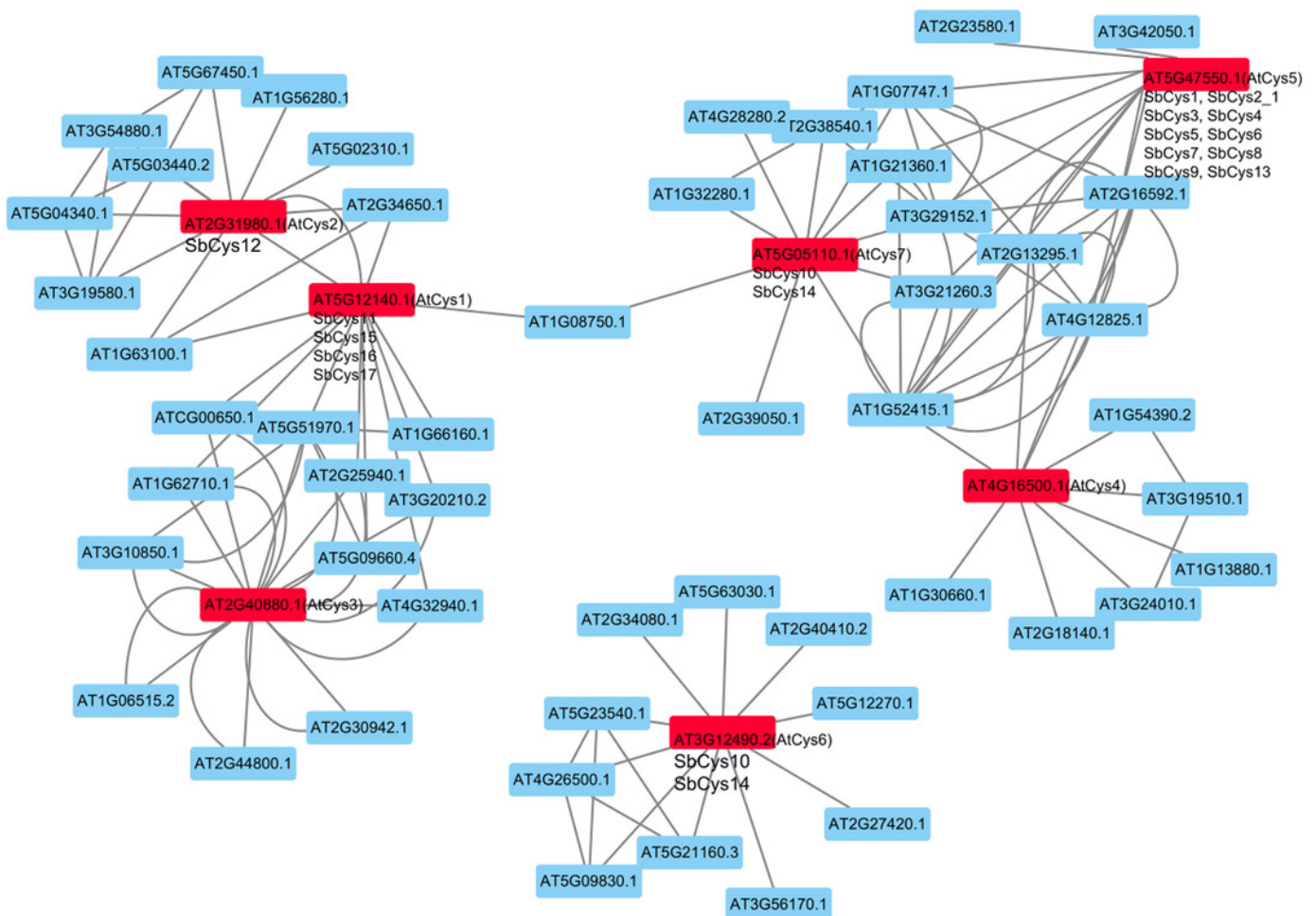


Figure 8

Hierarchical clustering of the expression profiles of *SbCys* genes in different tissues .

Different tissues are exhibited below each column. Root, shoot, and whole organism belonged to vegetable tissues were collected at 14 days after Sorghum seed germination. Reproductive tissues included embryo , endosperm and pericarp were collected at 20 days after pollination; pollens at booting stage; Inflorescences based on sizes: 1-5 mm, 5-10 mm, and 1-2 cm. Log transform data was used to create the heatmap. The scale bar represented the fold change (color figure online). Blue blocks represented the lower expression level and red blocks represented the higher expression level.

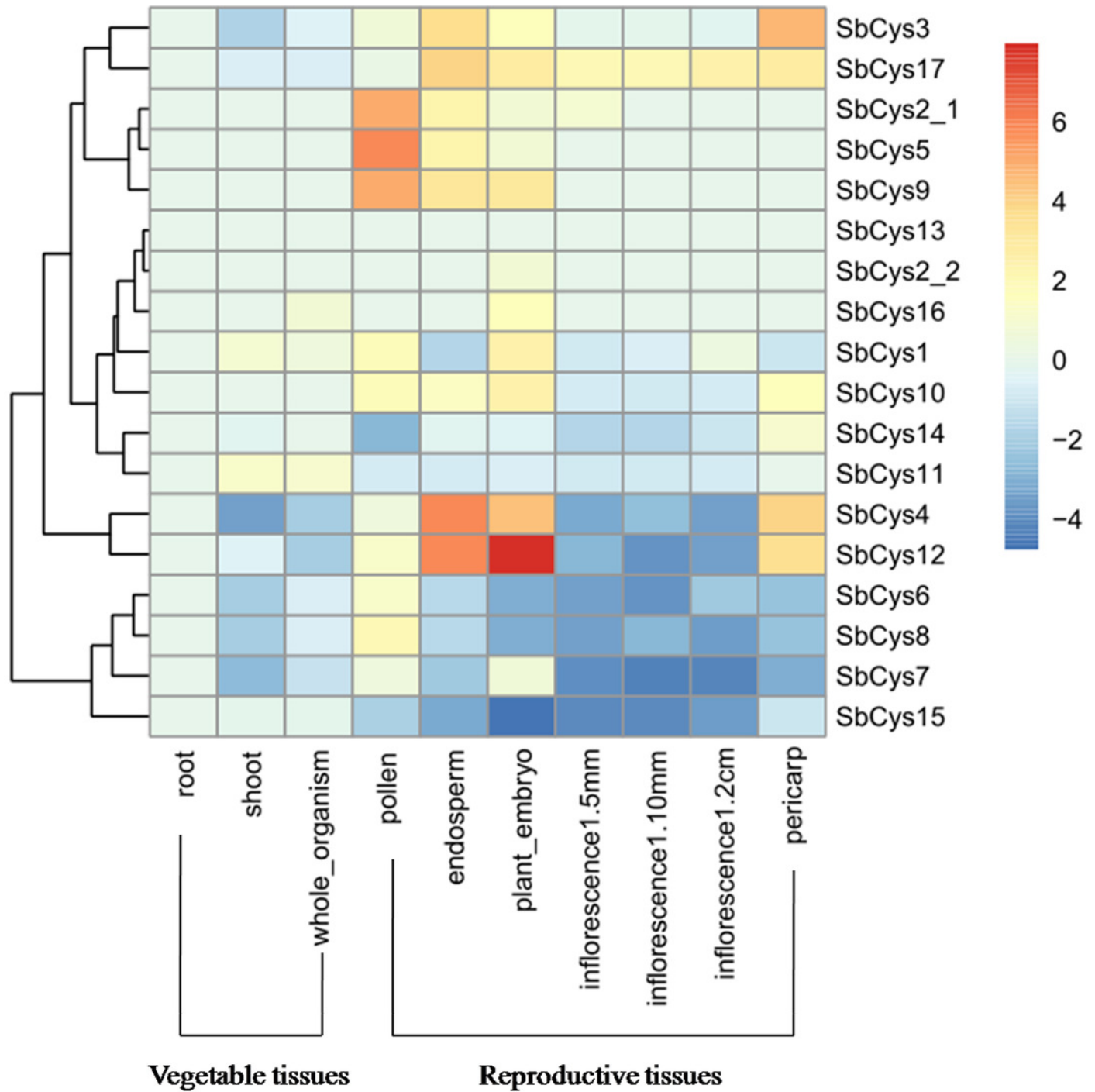


Figure 9

Hierarchical clustering of the expression profiles of *SbCys* genes under biotic stresses.

(A) The expression changes in *SbCys* genes at 0, 12, and 24 hours with *Bipolaris sorghicola* infection. (B) The expression changes of *SbCys* genes at 5, 10, 15 days with sugarcane aphid infestation. Log transform data was used to create the heatmap. The scale bar represents the fold change (color figure online). Blue blocks indicate low expression and red blocks indicate high expression (color figure online).

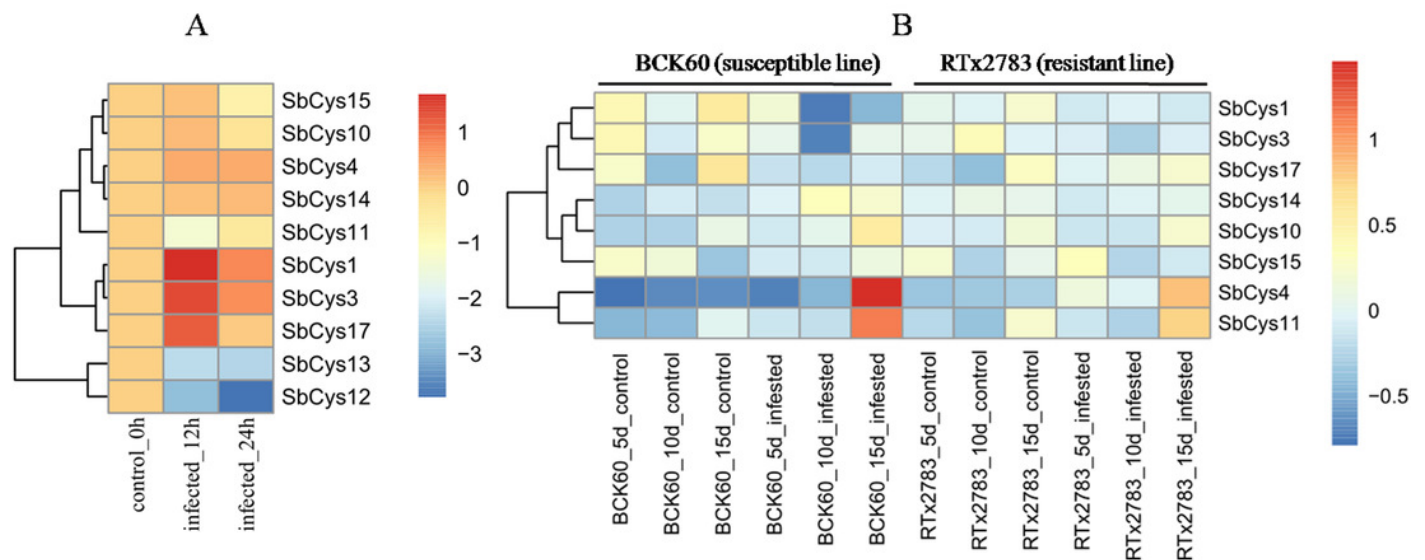


Figure 10

Expression profiles of *SbCys* genes at 5, 10, and 15 days with sugarcane aphid infection.

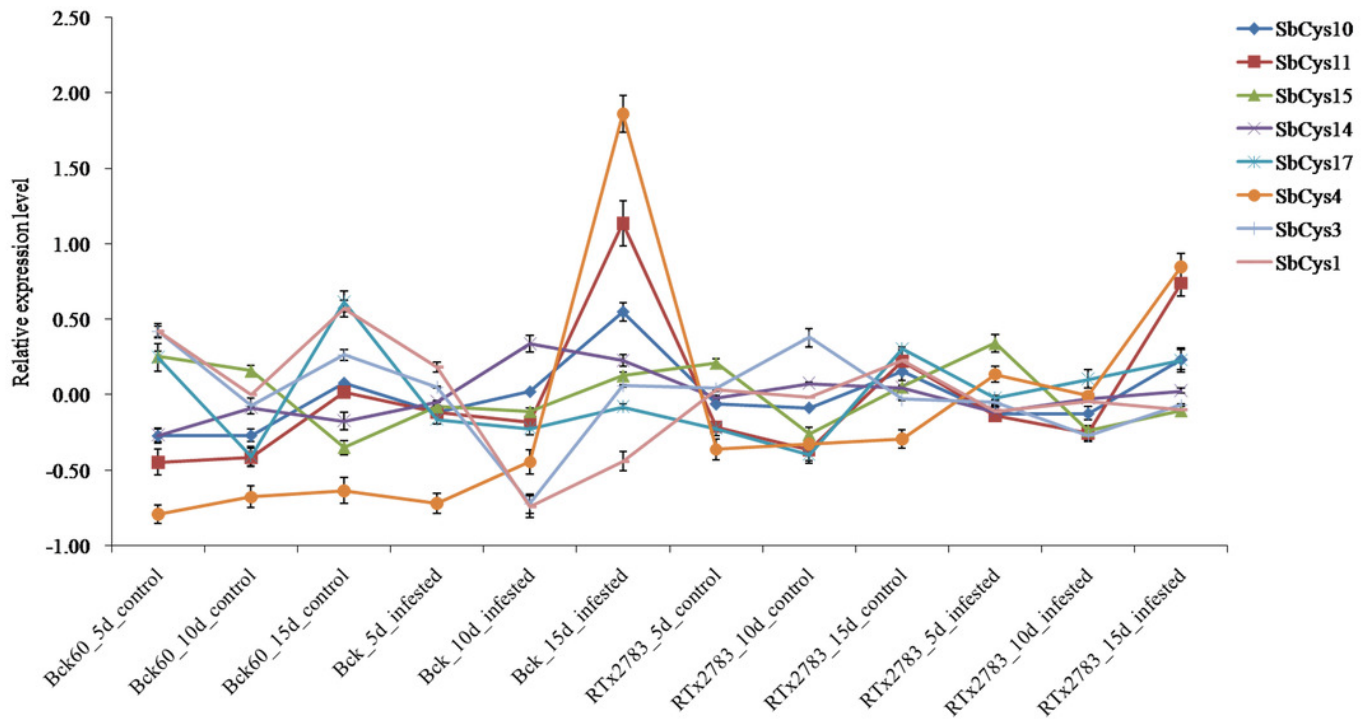


Figure 11

Expression patterns of *SbCys* genes under (A) dehydration (PEG 6,000) treatment, (B) salt shock (NaCl) treatment, and (C) ABA treatment.

qRT-PCR was used to investigate the expression levels of each *SbCys* gene. To visualize the relative expression levels data, 0 h at each treatment was normalized as “1”. * indicated significant differences in comparison with the control at $p \leq 0.05$. ** indicated significant differences in comparison with the control at $p \leq 0.01$.

